

Variable impairment of platelet functions in patients with severe, genetically linked immune deficiencies

Magdolna Nagy¹, Tom G. Mastenbroek^{1*}, Nadine J.A. Mattheij^{1*}, Susanne de Witt¹, Kenneth J. Clemetson,² Janbernd Kirschner³, Ansgar S. Schulz⁴, Thomas Vraetz⁵, Carsten Speckmann⁶, Attila Braun⁷, Judith M.E.M. Cosemans¹, Barbara Zieger^{6*} and Johan W.M. Heemskerk^{1*}

¹Department of Biochemistry, Cardiovascular Research Institute Maastricht (CARIM), Maastricht University, Maastricht, The Netherlands

²Department of Haematology, Inselspital, University of Bern, CH-3010 Bern, Switzerland

³Department of Neuropediatrics and Muscle Disorders, Medical Center, University of Freiburg, Freiburg, Germany

⁴Department of Pediatrics and Adolescent Medicine, University Medical Centre Ulm, Ulm, Germany

⁵Department of Pediatrics and Adolescent Medicine, Medical Center-University of Freiburg, Faculty of Medicine, Germany

⁶Center for Chronic Immunodeficiency and Department of Pediatrics and Adolescent Medicine, Medical Centre, University of Freiburg, Freiburg, Germany

⁷Institute of Experimental Biomedicine, University Hospital and Rudolf Virchow Centre, University of Würzburg, Würzburg, Germany

*TGM, NJAM, BZ and JWMH contributed equally to this work.

Running title: Platelet function in genetic immune deficiencies

Correspondence: Johan W. M. Heemskerk, PhD, Dept. of Biochemistry, CARIM, Maastricht University, P.O. Box 616, 6200 MD Maastricht, the Netherlands. Tel. +31-43-3881671, e-mail: jwm.heemskerk@maastrichtuniversity.nl

Word count: Abstract: 246 , Main text: 3947

Number of figures/tables: 6 figures, 2 tables

Supplementary file: 1 pdf file (methods, 5 figures and 1 table)

Acknowledgments: Financial support from the Netherlands Centre for Translational Molecular Medicine (CTMM, MICRO-BAT), the Interreg V Euregio Meuse-Rhine program (Poly-Valve), Dutch Heart Foundation (2015T79 to T.G.M., and J.M.E.M.C.) and the Netherlands Organization for Scientific Research (NWO Vidi 91716421 to J.M.E.M.C.).

Abstract

In patients with dysfunctions of the Ca^{2+} channel ORAI1, stromal interaction molecule 1 (STIM1) or integrin-regulating kindlin-3 (FERMT3), severe immunodeficiency is frequently linked to abnormal platelet activity. In this paper, we studied in nine rare patients, including relatives, with confirmed genetic mutations of ORAI1, STIM1 or FERMT3, platelet responsiveness by multi-parameter assessment of whole blood thrombus formation under high-shear flow conditions. In platelets isolated from 5 out of 6 patients with ORAI1 or STIM1 mutations, store-operated Ca^{2+} entry (SOCE) was (in)completely defective compared to control platelets. Parameters of platelet adhesion and aggregation on collagen microspots were impaired for 4/6 patients, in part related to a low platelet count. For 4 patients, platelet adhesion/aggregation and procoagulant activity on VWF/rhodocytin and VWF/fibrinogen microspots were impaired, independently of platelet count and partly correlated with SOCE deficiency. Measurement of thrombus formation at low shear rate confirmed a larger impairment of platelet functionality in the ORAI1 patients than in the STIM1 patient. For 3 patients/relatives with a FERMT3 mutation, all parameters of thrombus formation were strongly reduced regardless of the microspot. Bone marrow transplantation, required by two patients, resulted in overall improvement of platelet function. We concluded that multiparameter assessment of whole-blood thrombus formation, in a surface-dependent way, can detect: (i) additive effects of low platelet count and impaired platelet functionality; (ii) aberrant ORAI1-mediated Ca^{2+} entry; (iii) differences in platelet activation between patients carrying the same ORAI1 mutation; (iv) severe platelet function impairment linked to a FERMT3 mutation and bleeding history.

Key words: FERMT3, ORAI1, platelets, store-operated calcium entry, STIM1

Introduction

Severe, genetically linked immunodeficiency can be accompanied by platelet function defects, especially in case of rare mutations in the *ORAI1*, *STIM1* and *FERMT3* genes on platelet properties, in spite of the solid evidence for a role of the mouse orthologues in arterial thrombosis.

In platelets and other blood cells, stromal interaction molecule 1 (STIM1) acts as a major Ca^{2+} sensor located in the endoplasmic reticulum. Upon lowering of the reticular Ca^{2+} concentration, it assembles with the ORAI1 Ca^{2+} (I_{CRAC}) channels in the plasma membrane to mediate store-operated Ca^{2+} entry (SOCE).¹⁻⁴ The conventional test for SOCE (*i.e.*, for STIM1 and ORAI1 activity) hence is to provoke depletion of the STIM1-linked Ca^{2+} store with the endoplasmic Ca^{2+} -ATPase inhibitor thapsigargin, and then measure Ca^{2+} entry through ORAI1 channels upon addition of extracellular CaCl_2 .^{5, 6}

Both ORAI1 and STIM1 have non-redundant roles in the patrolling and defense functions of white blood cells. In platelets, ORAI1 as well as STIM1 are considered to enhance the Ca^{2+} signal generation, especially induced by protein tyrosine kinase-linked receptors, such as glycoprotein VI (GPVI). In mouse, both ORAI1 and STIM1 are implicated in hemostasis and arterial thrombus formation.⁷⁻¹⁰ Murine knockout studies have indicated that the ORAI1-STIM1 Ca^{2+} signaling contributes to multiple platelet activation processes, such as adhesiveness via integrin activation, granule release, aggregation of platelets, and procoagulant activity.^{8, 11, 12} However, in humans, the consequences of defective ORAI1 or STIM1 activity in platelets have only poorly been investigated.

In humans, dysfunctional mutations in the *ORAI1* or *STIM1* genes are very rare.¹³ The patients described with such mutations usually suffer from severe immunodeficiency, congenital myopathy, ectodermal dysplasia or other Ca^{2+} -linked abnormalities.¹⁴⁻¹⁶ The immune deficiency can be attributed to the loss-of-function of leukocyte and lymphocyte subsets. Given the severity of the symptoms often already at a young age, these patients are commonly treated by allogeneic hematopoietic stem cell transplantation. The few patients described do not have an overt bleeding history, although they may periodically show autoimmune thrombocytopenia.¹⁶

Leukocyte adhesion deficiency type III (LAD-III) forms another severe immune disease, in this case accompanied by epistaxis or petechiae. It is associated with dysfunctional mutations in the *FERMT3* gene of the integrin-regulation protein, kindlin-3.¹³ LAD-III patients present with normal platelet count, but impaired platelet adhesion, which may explain the bleeding symptoms.^{17, 18} Also these patients may require hematopoietic stem cell transplantation during childhood.¹⁹

Recently, we developed a microspot-based assay for multiparameter assessment of whole-blood thrombus formation under flow conditions.²⁰ This assay proved to be valuable to characterize platelet count and function abnormalities in patients with a variety of genetic bleeding disorders. Here, we used this integrative method to investigate overall platelet functions in nine patients with severe immunodeficiencies, including parents, with a confirmed dysfunctional mutation in *ORAI1*, *STIM1* or *FERMT3*. For two patients, we also investigated effects of bone marrow transplantation. The results suggest a variable phenotypic penetrance on platelet properties in patients and relatives carrying those mutations.

Methods

Patients and controls

Blood was drawn from patients and healthy controls after full informed consent (Helsinki declaration). The studies were approved by the local Medical Ethics Committees. Healthy controls had normal blood cell counts, were devoid of anti-platelet medication for at least 2 weeks, and did not have a known history of bleeding or immunodeficiency.

Blood samples from patients with immunodeficiency and their parents (all genotyped) were collected at the Department of Pediatrics and Adolescent Medicine, University Medical Center in Freiburg, and at the Children's Hospital, University of Ulm (Table 1). Simultaneously, blood samples were taken from healthy donors, serving as daily travel controls. Relevant patient characteristics, including identified mutations and the clinical history are summarized in Table 1. Patient P1 showed homozygosity in the R91W mutation in the ORAI1, known to be linked to severe combined immunodeficiency and defective T cell Ca^{2+} signaling.¹ Heterozygosity in this mutation was confirmed for both parents (P2 and P3). Patient P4 carried a heterozygous G98S mutation in ORAI1, which was confirmed in the mother (P5). This mutation is reported to be linked to tubular aggregated myopathy-2.²¹ Patient P6 carried a heterozygous R429C mutation of STIM1, which is also linked to T cell immunity.²² Patient P7 suffered from severe immunodeficiency, linked to a homozygous R573X mutation in kindlin-3 encoded by the *FERMT3* gene. The two parents (P8 and P9) were heterozygous for this mutation. Two of the patients with severe immunodeficiency, P1 and P7, were eligible for bone marrow transplantation. Blood samples in these cases were obtained before and at 2 or 3 months after transplantation, respectively. The volumes of blood available for investigation were limited due to the young age of the patients.

Platelet Ca^{2+} responses

Rises in cytosolic $[\text{Ca}^{2+}]_i$ were measured in platelets after loading with Fura-2 acetoxymethyl ester (2.5 μM) by calibrated ratio fluorometry.²³ Data are presented as nM increases in cytosolic $[\text{Ca}^{2+}]_i$.²⁴

Multiparameter thrombus formation on microspots under flow

Whole blood thrombus formation was assessed under flow conditions, basically as described before.²⁰ In brief, blood samples (0.5 mL) were recalcified in the presence of thrombin inhibitors, and perfused over a coverslip coated with three microspots (spot 1: type I collagen, spot 2: VWF/rhodocytin, spot 3: VWF/fibrinogen) in a transparent parallel-plate perfusion chamber. Perfusion was at high wall-shear rate of 1600 s^{-1} for 3.5 min, or at low shear rate of 150 s^{-1} for 6.0 min. The thrombi formed on the microspots were immediately post-stained with FITC-labeled anti-fibrinogen mAb (1:100), FITC-anti-CD62P mAb (25 $\mu\text{g/mL}$) and AF647-annexin A5 (0.25 $\mu\text{g/mL}$). Representative brightfield and fluorescence images were captured from each microspot in real-time without fixation. Duplicate runs were performed, whenever possible. Analysis of brightfield and fluorescence images, giving 7 parameters per microspot, was performed with predefined scripts in Fiji software.²⁵ (Un)supervised heatmaps using scaled parameters (range 0-10) of thrombus formation were constructed in R.

Statistics

Significance of differences was determined with the paired sample t test (intervention

effects) and by principal component analysis (PCA), using the statistical package for social sciences (SPSS, version 11.0).

A detailed description of the methods is available in the *Online Supplementary Appendix*.

Results

Variable aberrances in SOCE in platelets from patients with ORAI1 or STIM1 mutations

Blood samples were obtained from three patients with a mutation in the Ca^{2+} flux-regulating proteins ORAI1 or STIM1, as well as from parents carrying the same mutation. For comparison, blood samples were also taken from two cohorts of healthy subjects, *i.e.* a group of normal home controls (HC1-12) and a group of normal travel controls (C1-6). Using Fura-2-loaded platelets, we first evaluated the alterations in Ca^{2+} signaling in response to the GPVI receptor agonist, convulxin, the PAR receptor agonist, thrombin, and the sarco/endoplasmic reticulum Ca^{2+} -ATPase (SERCA) inhibitor, thapsigargin. In each case, the platelets were first stimulated with agonist in Ca^{2+} -free medium, after which extracellular CaCl_2 was added to measure secondary Ca^{2+} entry.

In comparison to control platelets, platelets from patient P1, carrying a homozygous ORAI1^{91W/W} mutation, responded normally to each agonist, but showed a substantially reduced Ca^{2+} entry following stimulation with convulxin but not thrombin (Figure 1A-B). Markedly, in the patient's platelets, Ca^{2+} entry after stimulation with thapsigargin - as a default condition for SOCE -, was completely abolished. This pointed to a complete absence of the STIM1-ORAI1 pathway, similarly as established for

platelets from STIM1- or ORAI1-deficient mice.^{7, 8} Flow cytometric evaluation indicated that convulxin-stimulated platelets from P1 showed a reduced PS exposure ($7\pm1\%$ vs. $28\pm2\%$ for control platelets, mean \pm SEM, $n=3$, $P<0.05$), but were not altered in integrin $\alpha_{IIb}\beta_3$ activation or P-selectin expression ($P>0.10$). Platelets from the patient's parents (both with confirmed heterozygosity) were diminished in SOCE, but to a different extent (Figure 2). Platelets from the mother (P2) showed a nearly annulled Ca^{2+} entry, whereas platelets from the father (P3) were less severely reduced, when compared to platelets from two cohorts of healthy controls. A second blood sample from patient P1 could be obtained at 2 months after bone marrow transplantation. In the platelets, we measured about 50% recovery in SOCE signal after thapsigargin stimulation (SOCE_{P1}: 22 nM vs. SOCE_{P1-BM}: 575 nM).

Platelets from a patient (P4), carrying a heterozygous mutation ORAI1^{89G/S} in the same protein region, responded differently. These platelets displayed a high SOCE signal (Ca^{2+} entry after thapsigargin). In contrast, platelets from parent P5 (also carrying the mutation) were greatly reduced in SOCE (Figure 2). This difference was confirmed for a second set of blood samples (not shown). A different picture was obtained with patient P6 with a heterozygous mutation in STIM1^{429R/C}.²² In these platelets, Ca^{2+} rises evoked by convulxin/ $CaCl_2$ or thrombin/ $CaCl_2$ were in the normal range, whereas SOCE after thapsigargin was completely abolished (Figure 3A-B).

Phenotypic analysis of platelets was also performed of a LAD-III patient (P7), carrying a homozygous FERMT3^{573X/X} mutation, and presenting with immunodeficiency and a history of bleeding.²⁶ Flow cytometry indicated near complete inability of integrin $\alpha_{IIb}\beta_3$ activation in response to receptor agonists, similarly as described for another patient carrying this mutation.²⁷ In platelets from the two heterozygous parents (P8, P9),

$\alpha_{IIb}\beta_3$ integrin activation was in the normal range (not shown).

Lower range blood cell counts in patients with ORAI1, STIM1 or FERMT3 mutations

Table 1 provides an overview of the clinical histories of patients including P1-9, and furthermore informs on the hematological parameters, determined in freshly isolated blood samples. In all patients, with the exception of P1 and P7, platelet counts were between 70 and 150 x 10⁹/L, which are slightly below the normal ranges as present in both control cohorts. In the majority of patients, also hematocrit levels were in the lower range of normal, *i.e.* between 0.31 and 0.42 L/L. After bone marrow transplantation (2-3 months), platelet count in P1 and P7 had restored to 74 and 168 x 10⁹/L, respectively.

Different patterns between patients of aberrant whole-blood thrombus formation at high shear rate

To obtain detailed insight into the hemostatic potential of the patients' platelets, whole-blood samples were used for multiparameter assessment of thrombus formation under flow at high wall-shear rate of 1600 s⁻¹. Samples from corresponding control subjects (C1-6) and home control subjects (HC1-12) were again used for comparison. This high-throughput method, previously established,²⁰ allowed simultaneous examination of platelet adhesion, aggregation and activation at three microspots: spot 1 with coated type I collagen (involving platelet receptors: GPIb-V-IX, GPVI and integrin $\alpha_2\beta_1$); spot 2 with coated VWF/rhodocytin (receptors GPIb-V-IX and CLEC-2); and spot 3 with coated VWF/fibrinogen (receptors GPIb-V-IX and $\alpha_{IIb}\beta_3$). From each microspot, microscopic brightfield images were recorded to assess platelet adhesion and aggregation

(parameters V1-4); in parallel, fluorescence images were recorded in three colors for detection of PS exposure, P-selectin expression and $\alpha_{IIb}\beta_3$ activation (parameters V5-7).

Representative examples of brightfield and fluorescence images from spot 1 are shown in Figure 4, for blood samples of control C2 and immunodeficient patients with ORAI1 or STIM1 mutation (P1, P4, and P6). Regarding the patient blood samples, the images show patterns of platelet adhesion, aggregation and activation that vary from normal to reduced. The same holds for spot 2 (VWF/rhodocytin) and spot 3 (VWF/fibrinogen) (see below).

A heatmap was constructed with data from all analyzed images (3 spots \times 7 parameters) for the cohort of 12 normal home controls (HC1-12), the 6 travel controls (C1-6), and the 9 individual patients/relatives with mutations in ORAI1 (P1-5), STIM1 (P6) or FERMT3 (P7-9), in which all values were normalized to a scale of 0-10 per parameter (Figure 5A). In the derived subtraction heatmap of Figure 5B, the patient data were expressed relative to those from the home controls. This subtraction confirmed an overall high similarity between the values of the two control groups (HC1-12 and C1-6), with the exception of a parameter reflecting platelet deposition on spot 2. Datasets for individual subjects C1-6 were within the normal ranges (not shown). This confirmed the usefulness of the multi-parameter test,²⁰ and underscored the quality of the analyzed blood samples. For each patient/relative, we arbitrarily set a relevant effect threshold, *i.e.* when outside the range of mean \pm 2 SD of the control group (HC1-12). This filter produced a 'relevant' subtraction heatmap, indicating distinct patterns of altered parameters of thrombus formation for individual patients P1-9 (Figure 5C).

Overall, Figure 5C underlines that multiple parameters on spot 1 were reduced for patients P2-5, whereas especially parameters on spots 2-3 were reduced for patients

P1 and P5. Interestingly, patient P4 carrying the assumed gain-of-function mutation ORAI1^{G98S} (but not relative P5 with low SOCE) showed a typical increase in platelet PS exposure. For the patient with homozygous FERMT3 mutation (P7), a more severe reduction on all three spots was seen in comparison to the two heterozygous relatives (P8-9).

Effects of low platelet count

Considering that whole-blood thrombus formation can be influenced by not only the inherited platelet disorder, but also a low platelet count,²⁸ the present heatmaps may reflect both platelet-related properties. To examine this in more detail, the subtraction heatmap data were extended with values of platelet count and SOCE. Unsupervised clustering of the extended dataset indicated that in particular spot 1, parameters (V1-4) clustered with platelet count, while spot 2 parameters (V3-5) and PS exposure (Sp1V5, Sp2V5) clustered with altered SOCE (Suppl. Figure 1).

As an alternative approach, we used the primary (non-normalized) data of thrombus formation (Sp1-3, V1-7), platelet count and SOCE for principal component analysis (PCA). This revealed a similar pattern, in that the majority of spot 1 parameters together with platelet count determined component 1, whereas most spot 2 parameters determined component 2 (Suppl. Figure 2A). Statistics (Pearson's regression coefficient) confirmed a correlation of spot 1 parameters with platelet count, and also a correlation of platelet PS exposure (Sp1V5, Sp3V5) with SOCE (Suppl. Figure 2B).

This information was then used to interpret the alterations in thrombus formation for individual patients (see clustered heatmap of Suppl. Figure 1). Concerning the patient (P1) with homozygous R91W mutation in ORAI1, with normal platelet count (207

$\times 10^9/L$) and near abolished SOCE, thrombus formation was near normal on spot 1 (collagen), but markedly reduced on spot 2 (VWF/rhodocytin) and spot 3 (VWF/fibrinogen). The impaired Ca^{2+} signal was linked to a low PS exposure on all spots (Suppl. Table1). On the other hand, for the patients P2 and P3 with heterozygous R91W mutation in ORAI1 (relatively low platelet counts of $115-156 \times 10^9/L$, and 20-60% of normal SOCE, respectively), especially parameters for spot 1 were below normal, with a reduced PS exposure.

Concerning patients P4 and P5 heterozygous for the G98S mutation in ORAI1 (low platelet counts of 70 and $114 \times 10^9/L$; 100% and 30% of normal SOCE, respectively), thrombus formation on spot 1 was reduced, while parameters of thrombus formation on spots 2-3 (including PS exposure) were only reduced for patient P5. In P4 (but not P5) a gain-of-function of Ca^{2+} channel activity was apparent from an increased PS exposure on spots 2-3. For patient P6, heterozygous for the R429C mutation in STIM1, thrombus formation on spot 1 (collagen) was normal in spite of the abolished SOCE. Together, this underlined the idea that a low platelet count rather than altered SOCE determines the thrombus formation on collagen, but not on the other surfaces.

Control experiments with reconstituted blood confirmed that, for control donors, lowering of the platelet count to $100 \times 10^9/L$ had a minor effect on particular parameters of thrombus formation limited to spot 1, whereas lowering to $50 \times 10^9/L$ affected thrombus formation on all spots 1-3 (Suppl. Figure 3). Taken together with the predictive effect of platelet count in the principal component analysis, this suggest that a relatively low count affects thrombus formation under flow more severely when combined with a reduced platelet functionality.

Patterns of aberrant whole-blood thrombus formation at low shear rate

Using remaining samples from patients/relatives P1-6, we further performed whole-blood flow measurements at a low shear rate of 150 s^{-1} . Subtraction heatmap analysis of the normalized parameter values, in comparison to control data from HC1-12 cohort, indicated for all patients with ORAI1 mutations (P1-5) a consistent pattern of reduced thrombus formation parameters on spot 1 (Suppl. Figure 4A-C). In particular for patients P2 and P3, markers of platelet activation appeared to be reduced (PS exposure, P-selectin expression and $\alpha_{\text{IIb}}\beta_3$ activation). Again, for patient P6 with STIM1 mutation, most parameters were unchanged.

Principal component analysis of the low shear data again pointed to a linkage of spot 1 parameters with platelet count and a linkage of Sp1V5 (PS exposure) with SOCE activity (Suppl. Figure 5A-B).

Partial recovery of whole-blood thrombus formation after bone marrow transplantation

Blood samples from two patients were also obtained after bone marrow transplantation (P1 after 2 months, P7 after 3 months), and employed for platelet activation and thrombus formation studies. Transplantation of patient P1 led to a partially recovered SOCE from 20 to 60% of normal (Figure 2). After transplantation, parameters of thrombus formation were particularly reduced on spot 1 (paralleling a reduction in platelet count from 207 to $74 \times 10^9/\text{L}$), but were unchanged for spot 2, and enhanced for spot 3 (Figure 6). Transplantation of patient P7 resulted in an overall improvement of most parameters on all spots (platelet count changing from 182 to $168 \times 10^9/\text{L}$).

Discussion

In the present study, we used a multiparameter test of whole-blood thrombus formation under flow conditions, as a proxy measurement of hemostatic activity,²⁰ to characterize quantitative and qualitative platelet abnormalities in rare patients and their relatives with severe immunodeficiencies, linked to signaling protein defects and mutations in the *ORAI1*, *STIM1* and *FERMT3* genes. So far, functional effects of the *ORAI1* and *STIM1* mutations have only been described for human immune cells or cell lines. Hence, the present data are the first to report on comparative alterations in platelet SOCE and platelet functions in as many as nine genotyped patients/relatives.

Aberrations in SOCE accompanied by mutations in *ORAI1* or *STIM1*

Earlier work with bone marrow chimeric mice with megakaryocytic deficiency in *Orai1* or *Stim1* demonstrated a prominent role of these Ca^{2+} -entry regulating proteins in platelet calcium homeostasis and activation, including PS exposure.^{11, 29} Our human data are compatible with these findings in that SOCE after thapsigargin or GPVI stimulation appeared to be impaired in platelets from patient P1 with a homozygous *ORAI1*^{W/W} mutation. A similar impairment of SOCE has been reported in platelets from *Orai1*^{R93W} mice, *i.e.* a loss-of-function mutation orthologous to the human *ORAI1* R91W variant.²⁹ Platelets from the latter mice showed a defect in Ca^{2+} fluxes and other responses, when triggered with low concentrations of (thrombin or collagen) receptor agonists. These platelets displayed normal aggregation under flow conditions, but a decreased procoagulant activity (PS exposure).²⁹

Relatives P2 and P3, heterozygous for the R91W mutation, showed about 20-

50% residual SOCE activity, which is compatible with co-expression of the non-mutated allele in the platelets. Interestingly, Ca^{2+} entry after thrombin stimulations remained unaffected in patients/relatives P1-3, which is explained by involvement of the SOCE-independent Ca^{2+} entry mechanism through TRPC6 channels.³⁰

On the other hand, the R98S mutation in ORAI1, with assumed gain-of-function,³¹ carried by patient P4, was not accompanied by altered SOCE activity after thapsigargin or GPVI stimulation, whereas SOCE was substantially reduced in the relative P5 (confirmed in two independent blood samples). The difference in SOCE activity between P4 and P5 might be explained by a different 'penetration' of the mutated allele in ORAI1 expression in megakaryocytes and platelets. However, an alternative explanation is the presence of other modifying genetic or acquired factors between P4 and P5, with possible effects on platelet SOCE activity, on which we can only speculate.

Concerning patient P6 with a heterozygous R429C mutation in STIM1, Ca^{2+} entry in platelets was impaired after thapsigargin, but not after GPVI or PAR1/4 stimulation. In mammalian cell lines, the R429 mutation modulates the C-terminal oligomerization and puncta formation of STIM1 with ORAI1.³² Our results suggest that, in platelets, this mutation strongly inhibits the interaction of STIM1 with ORAI1 after full Ca^{2+} store depletion, such as provoked by thapsigargin.

Altered platelet functions in thrombus formation accompanied by mutations in ORAI1, STIM1 or FERMT3

Previous murine studies have pointed out that deficiency in platelet ORAI1 or STIM1 led to a moderately reduced collagen-dependent thrombus formation with minimal effect on bleeding,^{8, 11} whereas murine deficiency in FERMT3 (kindlin-3) resulted in impaired

thrombus formation and a clear bleeding phenotype.³³ Furthermore, both ORAI1-deficient and ORAI1^{R93W} mouse platelets were found to be partly defective in procoagulant activity (PS exposure), along with the annulled SOCE activity.^{8, 11, 29}

In the present study, we observed even more variable platelet phenotypes in the nine patients/relatives with a mutation in ORAI1, STIM1 or FERMT3. Heatmap analysis indicated extensive but distinct patterns of reduced thrombus formation between patients, compared to blood from cohorts of healthy control subjects. Blood analysis further indicated that most patients/relatives carrying such a mutation had platelet counts below or near the lower range of normal. Low platelet count was found to correlate with low thrombus formation parameters, especially on spot 1. By comparison with flow studies using blood from healthy controls at lower counts, it appears that mild thrombocytopenia can lead to a more severe reduction in thrombus formation if combined with lower platelet functionality. Mild thrombocytopenia for patients with a loss-of-function mutation in ORAI1 or STIM1 has been reported before.¹⁶ So far, published papers on patients with a FERMT3 mutation do not report on thrombocytopenia.^{26, 27}

Because of the relatively large number of patients in our study, we were able to separate the thrombus formation parameters linked to qualitative or quantitative platelet defects. Both unsupervised clustering of the heatmap data and principal component analysis of the raw data indicated that mostly thrombus parameters on spot 1 (collagen; platelet receptors GPIb-V-IX, GPVI, $\alpha_2\beta_1$) showed a dependency on platelet count, whereas those of spot 2 (VWF/rhodocytin; receptors GPIb-V-IX, CLEC-2) and spot 3 (VWF/fibrinogen; receptors GPIb-V-IX, $\alpha_{IIb}\beta_3$) were not dependent of platelet count.

Markedly, this was true for both the high-shear and low-shear flow tests. An explanation for this finding is that, with collagen as a relatively strong agonist for GPVI, on spot 1 platelet delivery (thus, count) rather than platelet activation is a limiting factor for thrombus-forming parameters. In contrast, the immobilized ligands of spots 2-3, being less platelet-stimulating, may more rely on full platelet activation including normal SOCE and $\alpha_{IIb}\beta_3$ integrin activation. Correlation analysis also indicated that PS exposure was a key parameter linked to SOCE, in agreement with earlier mouse data.^{10, 11}

Improved platelet functions after bone marrow transplantation

Bone marrow transplantation of patient P1 (ORAI1^{WW}), 2 months before, resulted in improved SOCE activity and normalized thrombus formation on spot 3 but not on spot 1 (linked to a low platelet count). Transplantation of P7 (FERMT3^{XX}), 3 months before, led to an overall improvement of thrombus formation parameters (at normal platelet count). The partial restoration of platelet count at 2 months post-transplantation is compatible with reports that a full normalization can take several months.^{26, 34}

Conclusive remarks

In Table 2, based on the relevant differential analysis of thrombus formation parameters (see Figure 5C), a summative overview is given per patient of alterations in: platelet adhesion/aggregation, integrin activation/secretion and procoagulant activity (phases 1-3). This approach is based on the rationale that this whole-blood flow assay senses additive effects of low platelet count and impaired platelet functionality. Table 2 shows for all patients/relatives with ORAI1 (R91W) mutation an overall defect in adhesion/aggregation, as well as a defect in procoagulant activity. It also underlines that

the assumed gain-of-function mutation ORAI1 (G98S) in patient P4 is accompanied by a typical increase in procoagulant activity (but not in relative P5 with low SOCE). Furthermore, in patients carrying the FERMT3 (R573X) mutation, all platelet responses appeared to be more severely reduced in case of homozygosity than of heterozygosity. This may be of clinical relevance, since only the homozygous carrier P7 had a history of bleeding (see Table 1).

Competing Interests: The authors have declared that no competing interests exist.

Author's contribution: MN performed experiments, analyzed data and drafted the manuscript. TM, NM, SdW performed experiments, analyzed data. KC provided essential materials. JK, AS, TV, CS and BZ recruited the patients. JC and AB contributed ideas and corrected the manuscript. BZ and JH designed the study, drafted and finalized the paper.

References

1. Feske S, Gwack Y, Prakriya M, et al. A mutation in Orai1 causes immune deficiency by abrogating CRAC channel function. *Nature*. 2006;441(7090):179-85.
2. Penna A, Demuro A, Yeromin AV, et al. The CRAC channel consists of a tetramer formed by STIM-induced dimerization of Orai dimers. *Nature*. 2008;456:116-20.
3. Luik RM, Wang B, Prakriya M, Wu M, Lewis RS. Oligomerization of STIM1 couples ER calcium depletion to CRAC channel activation. *Nature*. 2008;454:538-42.

4. Soboloff J, Rothberg BS, Madesh M, Gill DL. STIM proteins: dynamic calcium signal transducers. *Nat Rev Mol Cell Biol.* 2012;13(9):549-65.
5. Varga-Szabo D, Braun A, Nieswandt B. STIM1 and Orai1 in platelet function. *Cell Calcium.* 2011;50:70-278.
6. Ambily A, Kaiser WJ, Pierro C, et al. The role of plasma membrane STIM1 and Ca^{2+} entry in platelet aggregation. STIM1 binds to novel proteins in human platelets. *Cell Signal.* 2014;26(3):502-11.
7. Varga-Szabo D, Braun A, Kleinschnitz C, et al. The calcium sensor STIM1 is an essential mediator of arterial thrombosis and ischemic brain infarction. *J Exp Med.* 2008;205(7):1583-91.
8. Braun A, Varga-Szabo D, Kleinschnitz C, et al. Orai1 (CRACM1) is the platelet SOC channel and essential for pathological thrombus formation. *Blood.* 2009;113(9):2056-63.
9. Gilio K, Harper MT, Cosemans JM, et al. Functional divergence of platelet protein kinase C (PKC) isoforms in thrombus formation on collagen. *J Biol Chem.* 2010;285:23410-9.
10. Van Kruchten R, Braun A, Feijge MA, et al. Antithrombotic potential of blockers of store-operated calcium channels in platelets. *Arterioscler Thromb Vasc Biol.* 2012;32(7):1717-23.
11. Gilio K, van Kruchten R, Braun A, et al. Roles of platelet STIM1 and Orai1 in glycoprotein VI- and thrombin-dependent procoagulant activity and thrombus formation. *J Biol Chem.* 2010;285(31):23629-38.
12. Heemskerk JW, Mattheij NJ, Cosemans JM. Platelet-based coagulation: different populations, different functions. *J Thromb Haemost.* 2013;11(1):2-16.
13. www.malacards.org. Malacards: human disease database. 2016.
14. Shaw PJ, Feske S. Regulation of lymphocyte function by ORAI and STIM proteins in infection and autoimmunity. *J Physiol.* 2012;590(17):4157-67.

15. Nakamura L, Sandrock-Lang K, Speckmann C, et al. Platelet secretion defect in a patient with stromal interaction molecule 1 deficiency. *Blood*. 2013;122(22):3696-8.
16. Lacruz RS, Feske S. Diseases caused by mutations in ORAI1 and STIM1. *Ann N Y Acad Sci*. 2015;1356:45-79.
17. Kuijpers TW, van de Vijver E, Weterman MAJ, et al. LAD-1/variant syndrome is caused by mutations in FERMT3. *Blood*. 2009;113:4740-6.
18. Van de Vijver E, De Cuyper IM, Gerrits AJ, et al. Defects in Glanzmann thrombasthenia and LAD-III (LAD-1/v) syndrome: the role of integrin $\beta 1$ and $\beta 3$ in platelet adhesion to collagen. *Blood*. 2012;119:583-6.
19. Stepensky PY, Wolach B, Gavrieli R, et al. Leukocyte adhesion deficiency type III: clinical features and treatment with stem cell transplantation. *J Pediatr Hematol Oncol*. 2015;37:264-8.
20. De Witt SM, Lamers MME, Swieringa F, et al. Identification of platelet function defects by multi-parameter assessment of thrombus formation. *Nat Commun*. 2014;5:4257.
21. Endo Y, Noguchi S, Hara Y, et al. Dominant mutations in ORAI1 cause tubular aggregate myopathy with hypocalcemia via constitutive activation of store-operated Ca^{2+} channels. *Hum Mol Genet*. 2015;24(3):637-48.
22. Fuchs S, Rensing-Ehl A, Speckmann C, et al. Antiviral and regulatory T cell immunity in a patient with stromal interaction molecule 1 deficiency. *J Immunol*. 2012;188:1523-33.
23. Feijge MA, van Pampus EC, Lacabartz-Porret C, et al. Inter-individual variability in Ca^{2+} signalling in platelets from healthy volunteers, relation with expression of endomembrane Ca^{2+} -ATPases. *Br J Haematol*. 1998;102:850-9.
24. Heemskerk JW, Vis P, Feijge MA, et al. Roles of phospholipase C and Ca^{2+} -ATPase in calcium responses of single, fibrinogen-bound platelets. *J Biol Chem*. 1993;268:356-63.
25. Schindelin J, Arganda-Carreras I, Frise E, et al. Fiji: an open-source platform for biological-image analysis. *Nat Meth*. 2012;9:676-82.

26. Crazzolaro R, Maurer K, Schulze H, et al. A new mutation in the KINDLIN-3 gene ablates integrin-dependent leukocyte, platelet, and osteoclast function in a patient with leukocyte adhesion deficiency-III. *Pediatr Blood Cancer*. 2015 Sep;62(9):1677-9.
27. Jurk K, Schulz AS, Kehrel BE, et al. Novel integrin-dependent platelet malfunction in siblings with leukocyte adhesion deficiency-III (LAD-III) caused by a point mutation in FERMT3. *Thromb Haemost*. 2010;103(5):1053-64.
28. Cauwenberghs S, Feijge MA, Theunissen E, et al. Novel methodology for the assessment of platelet transfusion therapy by measuring increased thrombus formation and thrombin generation. *Br J Haematol*. 2007;136:480-90.
29. Bergmeier W, Oh-Hora M, McCarl CA, et al. R93W mutation in Orai1 causes impaired calcium influx in platelets. *Blood*. 2009;113(3):675-8.
30. Hassock SR, Zhu MX, Trost C, Flockerzi V, Authi KS. Expression and role of TRPC proteins in human platelets: evidence that TRPC6 forms the store-independent calcium entry channel. *Blood*. 2002;100(8):2801-11.
31. Bohm J, Bulla M, Urquhart JE, et al. ORAI1 mutations with distinct channel gating defects in tubular aggregate myopathy. *Hum Mutat*. 2017;38(4):426-38.
32. Maus M, Jairaman A, Stathopoulos PB, et al. Missense mutation in immunodeficient patients shows the multifunctional roles of coiled-coil domain 3 (CC3) in STIM1 activation. *Proc Natl Acad Sci USA*. 2015;112(19):6206-11.
33. Moser M, Nieswandt B, Ussar S, Pozgajova M, Fassler R. Kindlin-3 is essential for integrin activation and platelet aggregation. *Nat Med* 2008;14(3):325-30.
34. Takami A, Shibayama M, Orito M, et al. Immature platelet fraction for prediction of platelet engraftment after allogeneic stem cell transplantation. *Bone Marrow Transplant*. 2007;39(8):501-7.

Subject(s)	Mutation	Platelet count (x 10 ⁹ /L)	MPV (fL)	Hematocrit (L/L)	Clinical history
HC1-12 (home C)	None assumed	166-390	9.1-12.1	0.36-0.49	None
C1-5 (travel C)	None assumed	156-291	9.0-11.6	0.36-0.40	None
P1 (child)	ORAI1 (R91W) W/W	207	n.d.	0.41	Immunodeficiency, myopathy, anhydrosis
P1 (BM)	BM transplanted	74 ⁺	8.9 ⁺	0.23 ⁺	Thrombocytopenia, stabilized myopathy
P2 (mother P1)	ORAI1 (R91W) R/W	115 ⁺	8.8 ⁺	0.36	Mild thrombocytopenia
P3 (father P1)	ORAI1 (R91W) R/W	156 ⁺	9.2	0.32 ⁺	No known history of bleeding
P4 (child)	ORAI1 (G98S) G/S	114 ⁺	7.7 ⁺	0.34 ⁺	Thrombocytopenia (recurrent), myopathy with tubular aggregates, anhydrosis
P5 (mother P5)	ORAI1 (G98S) G/S	70 ⁺	9.2	0.37	Thrombocytopenia, myopathy with tubular aggregates, anhydrosis
P6 (adult)	STIM1 (R429C) R/C	150	n.d.	n.d.	No known history of bleeding
P7 (child)	FERMT3 (R573X) X/X	182	7.5 ⁺	0.31 ⁺	Immunodeficiency, severe vaginal bleeding, leukocytosis
P7 (BM)	BM transplanted	168	6.0 ⁺	0.33 ⁺	No known clinical symptoms
P8 (father P7)	FERMT3 (R573X) R/X	126 ⁺	8.3	0.42	No known history of bleeding
P9 (mother P7)	FERMT3 (R573X) R/X	142 ⁺	6.8 ⁺	0.39	No known history of bleeding

+ Outside of normal range

Table 1. Subject characteristics. Abbreviations: MPV, mean platelet volume; n.d., not determined.

Subject	Mutation	SOCE	Sum	Phase1	Phase2	Phase3
HC1-12	None	o	0	0.00	0.00	0.00
C1-6	None	o	-1	0.00	0.00	-0.33
P1	ORAI1 (R91W) W/W	--	-10	-0.50	-0.17	-1.00
P2	ORAI1 (R91W) R/W	--	-8	-0.42	-0.17	-0.67
P3	ORAI1 (R91W) R/W	-	-10	-0.50	-0.33	-0.67
P4	ORAI1 (G98S) G/S	o	-4	-0.50	0.00	0.67
P5	ORAI1 (G98S) G/S	-	-13	-0.83	-0.33	-0.33
P7	FERMT3 (R573X) X/X	n.d.	-21	-1.00	-1.00	-1.00
P8	FERMT3 (R573X) R/X	n.d.	-14	-0.50	-0.83	-1.00
P9	FERMT3 (R573X) R/X	n.d.	-12	-0.42	-0.83	-0.67

Table 2. Overall comparison of defective SOCE and impairment in thrombus formation of individual patients. For indicated patients, measurements of SOCE (see Figure 2) and differential heatmap data relative to control cohort HC1-12 (see Figure 5C) were tabled to obtain an overview of the changes in platelet function. For thrombi (1600 s^{-1}) formed on the three microspots (Sp1-3), all parameters (V1-7) were scored as within normal range (0), decreased (-1) or increase (+1). Per patient, summed scores are indicated (column 'Sum'). In addition, fractions of altered scores are indicated for three phases of thrombus formation. Phase 1 refers to platelet adhesion and aggregation (Sp1-3, V1-4), phase 2 to platelet integrin activation and granule secretion (Sp1-3, V6-7), and phase 3 to platelet procoagulant activity (Sp1-3, V5).

Legends to figures

Figure 1. Defective Ca^{2+} entry in platelets from a patient with a homozygous R91W mutation in ORAI1. Fura-2-loaded platelets from patient P1 ($\text{ORAI1}^{\text{W/W}}$) and travel control C1 were used, suspended in Hepes buffer with 0.1 mM EGTA. Rises in cytosolic Ca^{2+} were measured in time upon stimulation with convulxin (Cvx, 50 ng/mL), thrombin (Thr, 4 nM) or thapsigargin (Thaps, 1.0 μM). After a defined time, CaCl_2 (2 mM) was added to induce Ca^{2+} entry. Representative traces (**A**) and quantification (**B**) of Ca^{2+} increases in platelets from control subject and patient P1. Note that the maximal Ca^{2+} rise in response to CaCl_2 following thapsigargin was used as a measure of SOCE capacity.

Figure 2. Variably defective Ca^{2+} entry in platelets from patients with $\text{ORAI1}^{\text{W/W}}$, $\text{ORAI1}^{\text{G/S}}$ or $\text{STIM1}^{\text{R/C}}$ mutations. Fura-2-loaded platelets in Hepes buffer with 0.1 mM EGTA were stimulated with thapsigargin (1.0 μM), and after a defined time with CaCl_2 (2 mM). Platelets were analyzed from 12 healthy home controls (HC1-12), 6 healthy travel controls (C1-6), and the indicated patients/relatives (P1-6). Platelets from patient P1 were also analyzed after bone marrow (BM) transplantation. Shown are maximal increases in Ca^{2+} . Dotted lines indicate range of SOCE levels (CaCl_2 -induced Ca^{2+} rise after thapsigargin) for platelets from home controls (mean \pm SD, for HC1-12).

Figure 3. Defective Ca^{2+} entry in platelets from a patient with a heterozygous R429C mutation in STIM1. Fura-2-loaded platelets from patient P6 ($\text{STIM1}^{\text{R/C}}$) and

travel control C6, suspended in Hepes buffer with 0.1 mM EGTA, were stimulated with convulxin (Cvx, 50 ng/mL), thrombin (Thr, 4 nM) or thapsigargin (Thaps, 1.0 μ M), after which CaCl_2 (2 mM) was given to induce Ca^{2+} entry. Representative traces (A) and quantification (B) of Ca^{2+} rises in platelets from control subject and patient P6.

Figure 4. Altered thrombus formation of blood from patients with ORAI1^{WW}, ORAI1^{G/S} or STIM1^{R/C} mutations. Whole blood from indicated control subjects and patients was perfused over three microspots (Sp1, collagen type I; Sp2, VWF/rhodocytin; Sp3, VWF/fibrinogen; downstream \rightarrow upstream) at wall-shear rate of 1600 s^{-1} . After 3.5 min of perfusion, brightfield images were taken from thrombi on all microspots, and platelets were stained for PS exposure (AF568-annexin A5), P-selectin expression (AF647 anti-CD62P mAb), and integrin $\alpha_{\text{IIb}}\beta_3$ activation (FITC anti-fibrinogen mAb). Shown are representative brightfield and fluorescence images at spot 1, obtained with blood from control C2 and patients P1, P4 and P6 (bars, 50 μm).

Figure 5. Integrated analysis of thrombus formation for patients with ORAI1, STIM1 or FERMT3 mutations. Thrombus formation on three microspots was measured with blood from home controls (HC1-12), travel controls (C1-6) and indicated patients/relatives with a genetic mutation in ORAI1 (P1-5), STIM1 (P6) or FERMT3 (P7-9), at wall-shear rate of 1600 s^{-1} , as for Figure 4. Coding of microspots: Sp1, collagen type I; Sp2, VWF/rhodocytin; Sp3, VWF/fibrinogen. Coding of outcome parameters: V1, thrombus morphological score (scale 0-5); V2, platelet surface area coverage (% SAC); V3 thrombus contraction score (scale 0-3); V4, thrombus multilayer score (scale 0-3);

V5, PS exposure (% SAC); V6, P-selectin expression (% SAC); V7, $\alpha_{IIb}\beta_3$ activation (% SAC). Data were scaled per parameter from 0-10. **(A)** Heatmap of scaled values for control groups HC1-12 and C1-6 (means); and of scaled values for individual patients (*) and relatives. **(B)** Subtraction heatmap of scaled values, compared to those from HC1-12. **(C)** Subtraction heatmap after filtering for differences considered to be relevant, *i.e.* outside the range of mean \pm 2 SD (HC1-12).

Figure 6. Altered thrombus formation after bone marrow transplantation.

Thrombus formation (1600 s^{-1}) on three microspots measured with blood from indicated home controls (HC1-12), travel controls (C1-6) and two patients P1 (ORAI1^{WW}) and P7 (FERMT3^{R/X}), both before (*) and after bone marrow transplantation (BMT). For description of microspots and parameters, as for Figure 4. Subtraction heatmap of scaled values after filtering for differences considered to be relevant, *i.e.* outside the range of mean \pm 2 SD (HC1-12).

Figure 1.

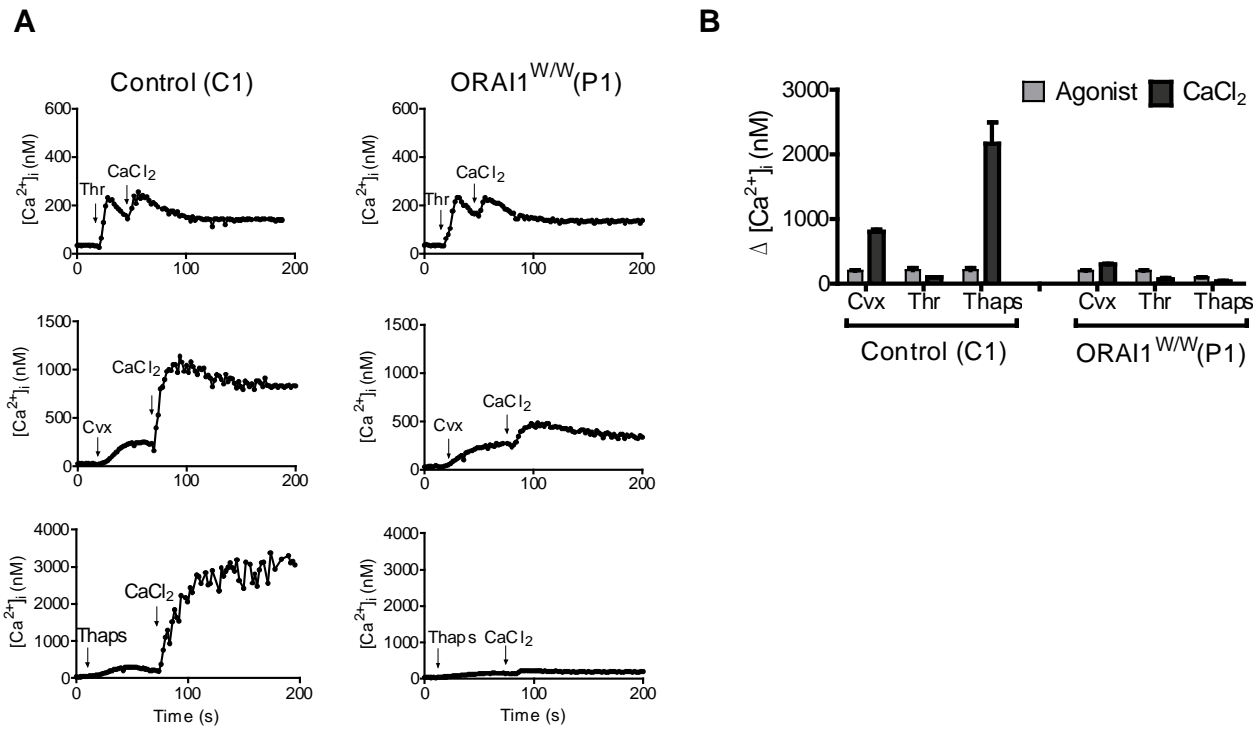


Figure 2.

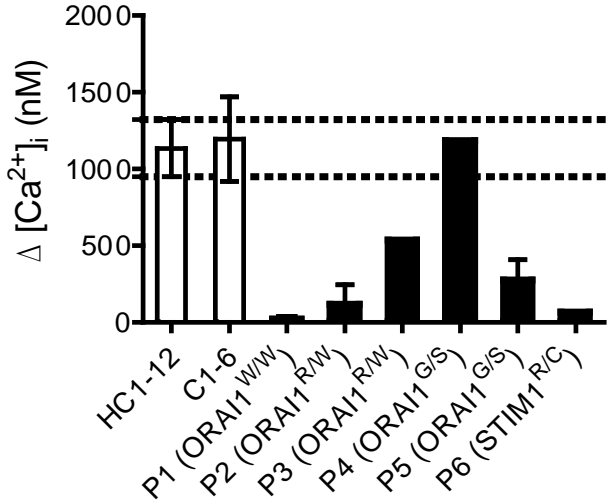


Figure 3.

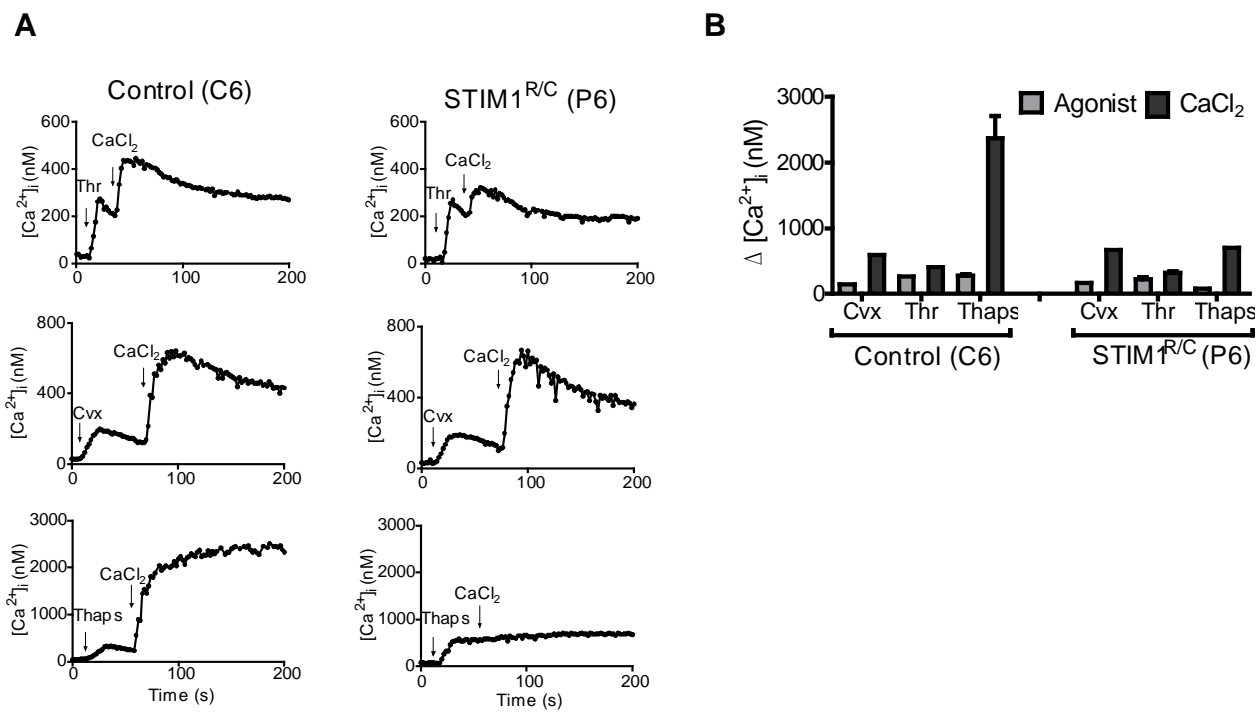


Figure 4.

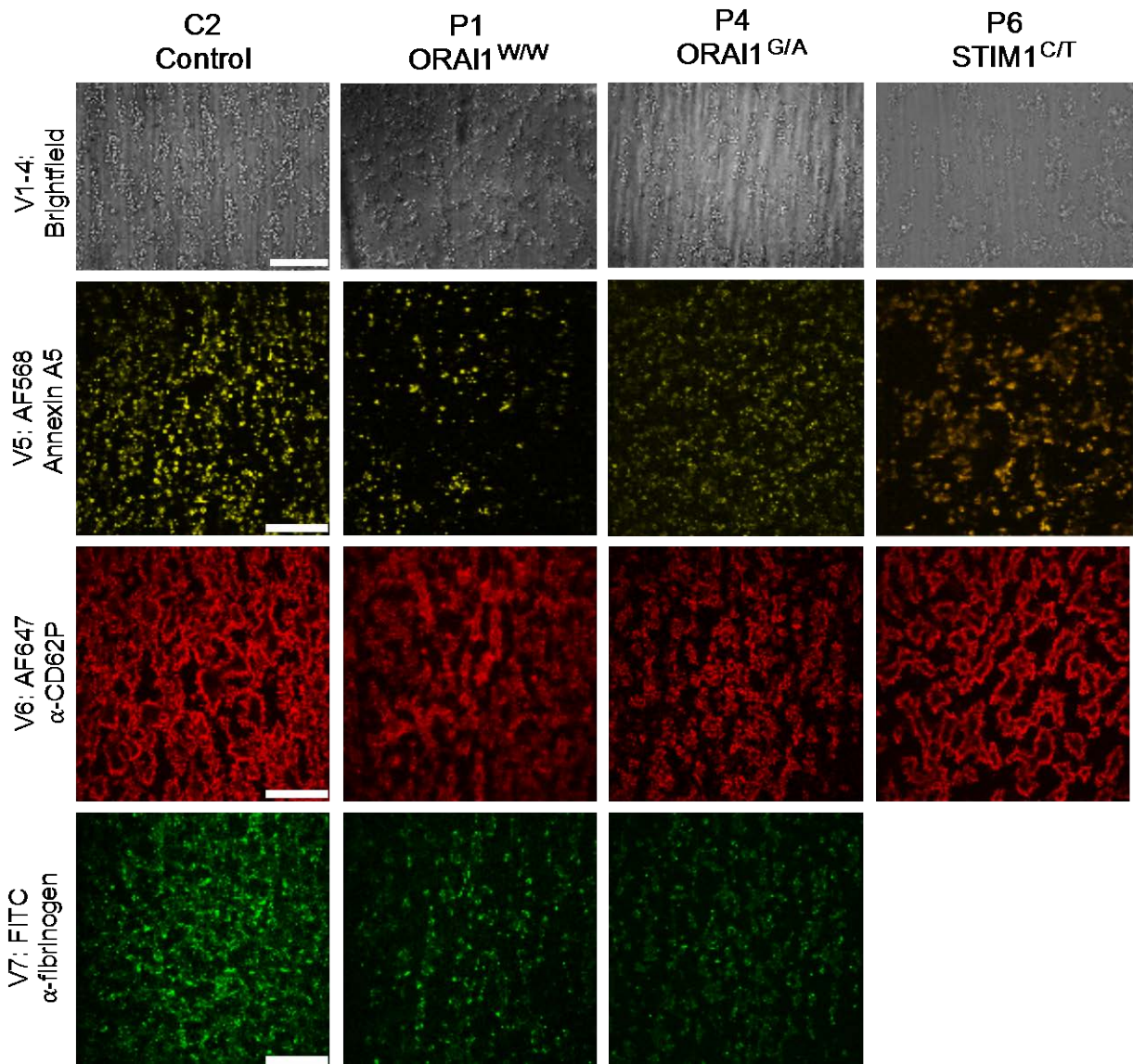
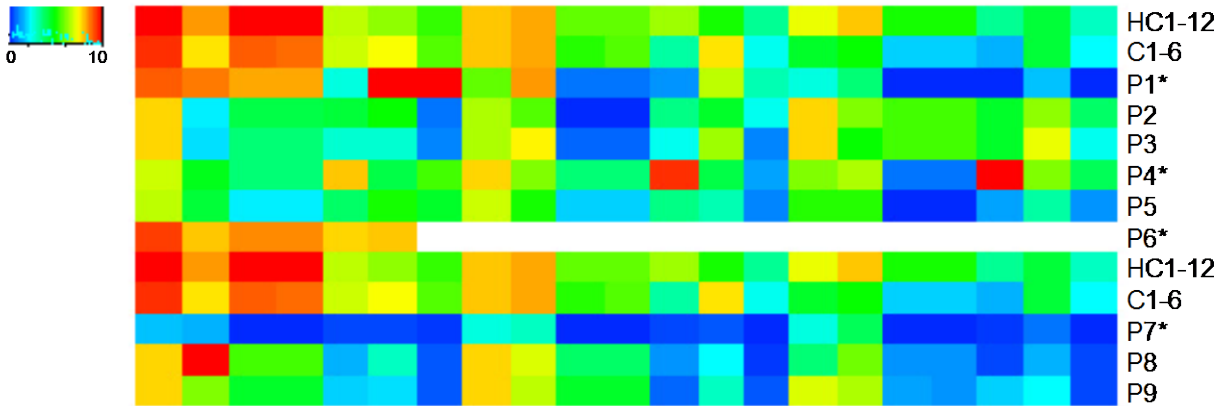
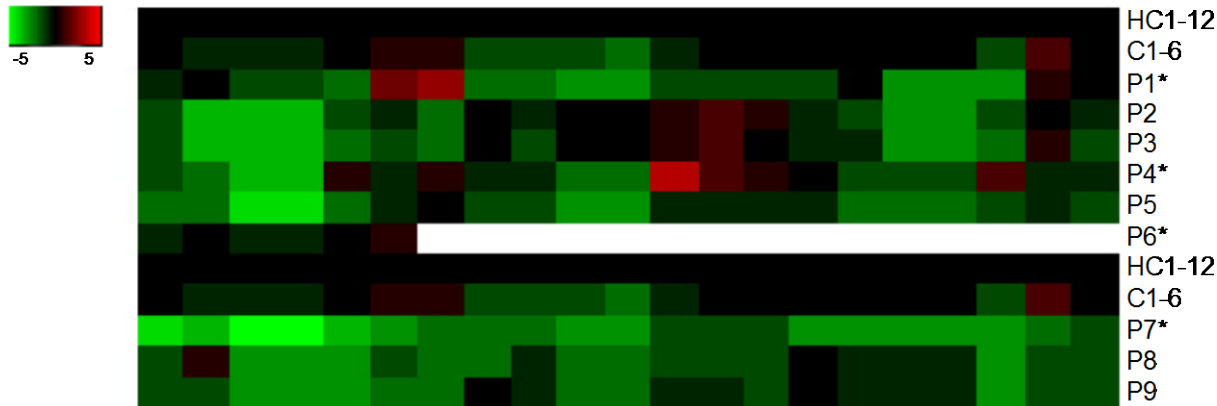


Figure 5.

A



B



C

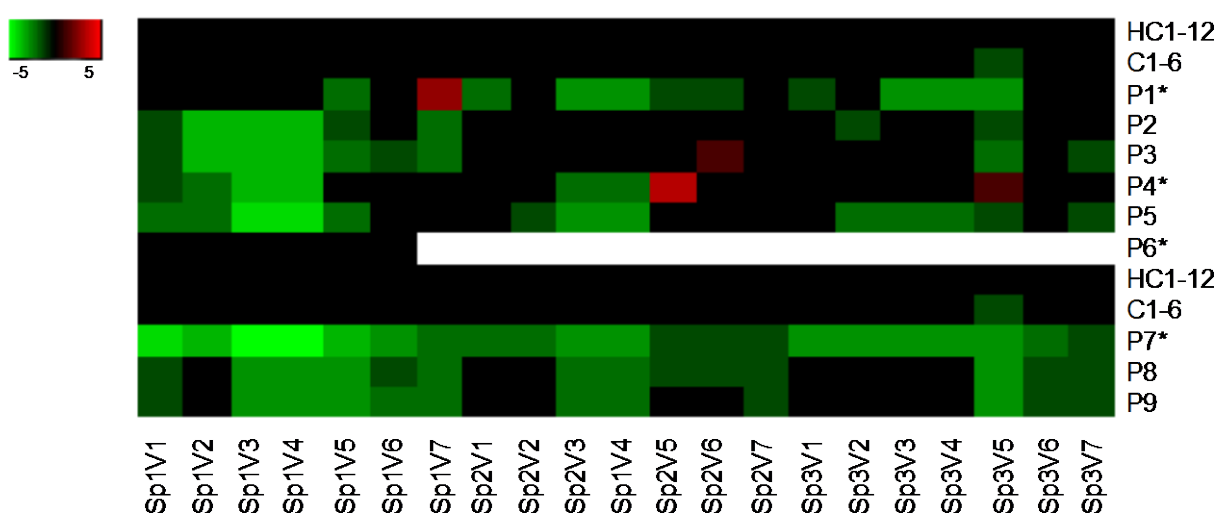


Figure 6.

